# **Unravelling the Internal Complexities of Molten Salts**

Ashok K. Adya, Ryuzo Takagi<sup>a</sup>, and Marcelle Gaune-Escard<sup>b</sup>

Division of Molecular & Life Sciences, School of Science & Engineering, University of Abertay Dundee, Bell Street, Dundee DD1 1HG, Scotland, U.K.

<sup>a</sup> Research Laboratory for Nuclear Reactors, Tokyo Institute of Technology, Ookayama, Meguro-ku, Tokyo 152, Japan

b IUSTI, CNRS – UMR 6595, Technopôle de Chateau-Gombert, 5 rue Enrico Fermi, 13453 Marseilles cedex 13, France

Z. Naturforsch. 53a, 1037-1048 (1998); received November 18, 1998

Much experimental and theoretical effort has gone into revealing the internal complexities of molten salts for the past two decades. In this paper we shall show how neutron diffraction and computer simulation techniques have helped in gaining a better understanding of these systems at the microscopic level. Firstly, a short review on the structure of molten halide systems as revealed by these techniques will be presented. Complementarity of using X-rays with neutrons and, some recent results on the structure of molten DyCl<sub>3</sub> obtained by combining neutron and X-ray diffraction with molecular dynamic simulations will be discussed. Neutron diffraction isotopic substitution techniques have played an important role in elucidating the interatomic structure of a diversity of molten salts. Pair distribution functions (PDFs), determined for a number of 1:1 and 2:1 halide melts, provided theorists with a critical test of their model potentials. It is now clear that for 1:1 molten systems theoretical models based on Fumi-Tosi potentials can adequately describe many of the structural features. Nevertheless, the challenge is two fold: (i) to determine real interatomic potentials for 2:1 and 3:1 molten systems capable of reproducing not only the microscopic structural details obtained at the partial PDF,  $g_{\alpha\beta}(r)$  level, but also their macroscopic behaviour and, (ii) to characterise the structure in binary molten salt mixtures.

Key words: Molten Salts; Structure; Neutron and X-ray Diffraction; Computer Simulations; Liquid State Structural Theory; Molten Halides.

#### Introduction

Extensive neutron diffraction (ND) studies of molten halides of alkali [1-10], alkaline earth and other metals with doubly charged ions [11–16] have been reported in literature where microscopic structural details at the partial pair distribution function (PDF) level were obtained by the isotopic substitution technique (NDIS). Since the two stable isotopes of chlorine (35Cl and 37Cl) have a large difference in neutron scattering lengths [17], it is not surprising that the most extensive data are for the chlorides on which we shall focus in this paper. A number of computer simulations [18–23], both molecular dynamics (MD) and Monte Carlo (MC), have also been reported on these materials, but in many cases the agreement between simulations and experiment is still far from quantitative. In comparison, there is a complete lack of structural information at the partial PDF level for molten 3:1 halides. Rare earths possess special properties such as high melting points, high densities, high thermal

Reprint requests to A. K. Adya; E-mail: A.K. Adya@tay.ac.uk Fax: +44 (0) 1382 308663.

Presented as an opening lecture at the European Research Conference on Molten Salts (Porquerolles 27 June – 3 July, 1998).

and electrical conductivities. They play a vital yet subtle role in everyday consumer products such as automotives, TV, low energy light bulbs, computers, fax, etc. and, in sophisticated industrial applications such as fibre optics, night vision devices, high performance alloys, nuclear fuels, etc. Rare earths are extracted and processed into metals, metal and magnet alloys, oxides, salts and various other forms. Their extraction and processing is based on molten salt technologies. There are several processes such as reprocessing of spent nuclear fuel, nuclear waste processing, etc. which are still under development. However, data on solid and molten lanthanide compounds are scarce and scattered. Intensive effort is being made currently at an international level both on research and development and on development of data banks such as NIST (National Institute of Standards and Technology, US Govt. Commerce), which is a Web-based Molten Salt Data Bank, and CODATA (Committee on Data for Science and Technology), a task group on molten salts. High quality structural information on lanthanide halides and their binary melts with alkali metal halides is lacking. As a part of this global activity, we have begun a programme of systematically investigating the structural and thermodynamic properties of these molten systems with a threepronged approach: (i) macroscopic behaviour of these systems is being investigated by studying thermodynamic (enthalpies and temperatures of formation, phase transitions and fusion, heat capacities, enthalpies of mixing, etc.) and other physico-chemical properties, (ii) their microscopic behaviour is investigated by studying structural properties and solid-solid structural phase transitions through diffraction techniques such as neutrons and X-rays, and spectroscopic techniques such as Raman spectroscopy and, (iii) MD computer simulations are then performed by refining the used model potentials in order to reproduce both their microscopic and macroscopic properties investigated experimentally.

### **Neutron Diffraction**

Neutrons are an ideal, unique and highly penetrating probe for the study of condensed matter via their non-destructive interaction with the nucleus rather than the electron cloud. This enables the technique of isotopic substitution (NDIS) to be employed whereby we can "sit on" a specific atom and view its atomic surroundings. Molten salts are representative examples of strongly coupled systems where both short- and long-ranged structures reflect the importance of chemical bonding. The NDIS technique allows us to obtain a detailed and unique structural information about short- and intermediate-range chemical order in these melts.

# Experimental

Neutron diffraction experiments were performed on the D4B hot source diffractometer of the high flux nuclear reactor at the Institut Laue Langevin (ILL), Grenoble (France). Scattering intensities were recorded covering an angular range in  $2\theta$  from  $1.5^{\circ}$  to  $143.8^{\circ}$ , i.e.,  $0.25 \le Q$  (Å<sup>-1</sup>) $\le 17.11$  where  $Q = (4\pi/\lambda) \sin \theta$  and,  $2\theta$  is the scattering angle for neutrons of wavelength  $\lambda$  (0.6983 Å).

### **Formalism**

The normalised intensity, I(Q) of coherently scattered radiation from a neutron diffraction experiment on a liquid melt  $MX_n$  containing two distinct species is given by

$$I(Q) \approx N \left[ \sum_{\alpha=1}^{2} c_{\alpha} \overline{b_{\alpha}^{2}} + F(Q) \right].$$
 (1)

The total structure factor F(Q) is a weighted average of the three partial structure factors  $S_{\alpha\beta}(Q)$ :

$$F(Q) = c_{\alpha}^{2} \overline{b}_{\alpha}^{2} [S_{\alpha\alpha}(Q) - 1] + c_{\beta}^{2} \overline{b}_{\beta}^{2} [S_{\beta\beta}(Q) - 1] + 2 c_{\alpha} c_{\beta} \overline{b_{\alpha} b_{\beta}} [S_{\alpha\beta}(Q) - 1],$$
(2)

where  $c_{\alpha}$  is the atomic fraction of the  $\alpha$  species,  $\bar{b}_{\alpha}$  and  $b_{\alpha}^{2}$  are respectively, the coherent mean and mean squared neutron scattering lengths for ions of type  $\alpha$ . Fourier transform of  $S_{\alpha\beta}(Q)$  yields the partial pair radial distribution functions (PDFs),  $g_{\alpha\beta}(r)$ :

$$[g_{\alpha\beta}(r)-1] = \frac{1}{2\pi^{2}\rho r} \int_{0}^{\infty} \cdot [S_{\alpha\beta}(Q)-1]Q\sin(Qr) dQ, (3)$$

where  $\rho$  is the average atomic number density, e.g.,  $\rho = 0.032$  atoms Å<sup>-3</sup> for DyCl<sub>3</sub> at 700 °C. The co-ordination number  $\bar{n}_{\alpha}^{\beta}$  for species of type  $\beta$  around a species of type  $\alpha$  in the range  $r_1 < r < r_2$  can be determined from the PDF,  $q_{\alpha\beta}(r)$ 

$$\bar{n}_{\alpha}^{\beta} = 4 \pi \rho c_{\beta} \int_{r_{1}}^{r_{2}} g_{\alpha\beta}(r) r^{2} dr.$$
(4)

The Fourier transform of F(Q) is G(r), the total radial distribution function, which can be written as a linear combination of all the three partial RDFs,  $g_{\alpha\beta}(r)$ :

$$G(r) = \sum_{\alpha=1}^{2} \sum_{\beta=1}^{2} c_{\alpha} c_{\beta} \overline{b_{\alpha}} \overline{b_{\beta}} [g_{\alpha\beta}(r) - 1]. \quad (5)$$

One or both of the scattering lengths in (2) can be changed by varying the isotopic composition of the sample and, if ND measurements are performed on three samples of different isotopic composition, it becomes possible in theory to extract the three  $S_{\alpha\beta}\left(Q\right)$  by solving an appropriate set of three simultaneous equations. However, it should be noted that, in practice, the extraction of partial structure factors  $S_{\alpha\beta}(Q)$ , especially the metal-metal term, is not always straightforward since its contribution to the total structure factors is often very small. Small differences in scattering lengths between some isotopes could also result in a poor conditioning of the separation matrix. Moreover, small systematic errors in the preparation/characterisation of samples and in data normalisation procedures could lead to significant amplification of experimental errors, thereby masking the signal with the

Diffraction data were collected for the three isotopic  $^{\text{nat}}\text{Dy}^{\text{nat}}\text{Cl}_3$ ,  $^{162}\text{Dy}^{\text{nat}}\text{Cl}_3$  and  $^{\text{nat}+162}\text{Dy}^{\text{nat}}\text{Cl}_3$  pure molten salt samples and two binary melts x DyCl<sub>3</sub>+(1-x) NaCl (x=0.25, 0.57) at 700 °C. Various correction procedures

Table 1. Structural properties of 1:1 molten metal chlorides by NDIS technique.

Salt (Ref.)	T/°C	$r_{c+-}^{a}$	$r_{+-}$	$n_{+-}$	$r_{s+-}^{b}$	$r_{c}^{a}$	r	n	$r_{s}^{b}$	$r_{c++}^{a}$	r <sub>++</sub>	n <sub>++</sub>	$r_{s++}^{b}$	r <sub>+</sub> /Å	r/r
LiCl [4]	685	-	2.3	3.5-4.0	2.41	_	3.7	_	3.62	_	3.7	_	1.2	0.60	1.61
LiCl [3]	685	2.9		5.5	2.41	1.9	_	_	3.62	2.0	_	_	1.2	0.60	_
NaCl [2]	875	2.09	2.78	4.0	2.76	3.19	3.9	13.3	3.62	3.19	3.96	13.0	1.9	0.95	1.41
KCl [5]	800	2.20	3.06	6.1	3.14	3.40	4.82	12.3	3.62	3.50	4.84	12	2.66	1.33	1.58
RbCl [6]	750	2.7	3.18	6.9	3.29	3.6	4.8	14	3.62	3.55	4.86	13	2.96	1.48	1.5
CsCl [7]	695	2.8	3.4	5.8	3.5	3.45	4.85	16.3	3.62	3.45	4.95	15.4	3.38	1.69	1.43
CsCl [5]	700	2.45	3.38	_	3.5	3.40	3.85	_	3.62	3.40	3.85	_	3.38	1.69	_
CuCl [8]	500	1.7	2.3	3	2.77	2.6	3.9	_	3.62	1.7	3.7	_	1.92	0.96	1.69
CuCl [9]	440	2.0	2.3	_	2.77	3.0	3.6	-	3.62	1.5	3.3	_	1.92	0.96	1.57
AgCl [10]	510	1.8	2.6	4.3	_	2.6	_	_	3.62	2.5	3.4	3.1	_	_	_
AgCl [10]	850	1.65	2.55	2.7	-	2.7	3.15	2.7	3.62	2.65	3.15	4.1	-	_	-

<sup>&</sup>lt;sup>a</sup>  $r_c$ =closest distance of approach; <sup>b</sup>  $r_s$ =sum of ionic radii.

were applied to obtain the total structure factors for the three pure samples, which were then used to extract the three partial structure factors  $S_{\mathrm{Dy-Dy}}(Q)$ ,  $S_{\mathrm{Dy-Cl}}(Q)$  and  $S_{\mathrm{Cl-Cl}}(Q)$ . The extracted  $S_{\mathrm{Dy-Dy}}(Q)$  was found to be unphysical, which could be due to one of the several reasons mentioned earlier. Such a situation is often dealt with by complex iterative procedures [7, 13]. In the present case, we combined two sets of neutron data in turn with the X-ray data of Mochinaga et al. [24–26] to extract the three partials in each case and found that one of our sample  $^{\mathrm{nat+162}}\mathrm{Dy^{\mathrm{nat}Cl_3}}$  had a normalisation error of ~5%. The details are described in [27]. The data were renormalised to extract the three partial structure factors  $S_{\alpha\beta}(Q)$ , and through Fourier transformation the three PDFs,  $g_{\alpha\beta}(r)$ .

### **Molecular Dynamics Simulations**

Molecular dynamics (MD) simulations on the pure and mixed binary melts were carried out by employing the Born-Mayer-Huggins pair potentials

$$\phi_{ij}(r) = \frac{z_i z_j e^2}{4 \pi \varepsilon_0 r} + b_{ij} \exp \left[\frac{\sigma_{ij} - r}{\rho}\right] - \frac{c_{ij}}{r^6}$$
 (6)

to describe the charge-charge, short range repulsion and dispersion interactions. The repulsion term is composed of  $\sigma_{ij}$ , the sum of ionic radii  $(r_i^0 + r_j^0)$ ,  $b_{ij}$ , a hardness parameter and  $\rho$ , a softness parameter. Two approaches were used: simulations performed by using the above pair potential alone, called the Rigid Ion Model (RIM), and those where the above potential was supplemented by taking into account the polarisation effects, called the Polarisable Ion Model (PIM) introduced recently by Wilson and Madden [28]. The details are described in [29–31].

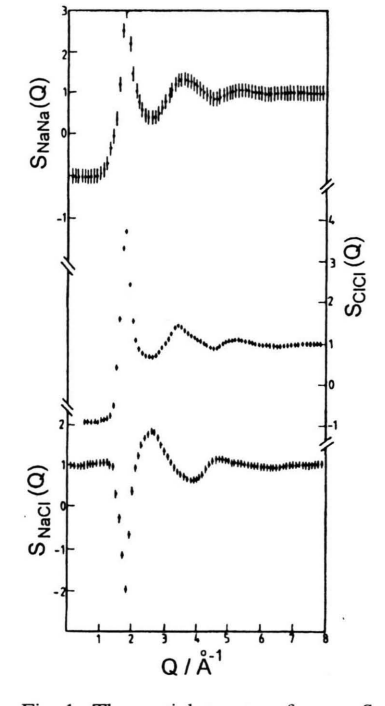


Fig. 1. The partial structure factors,  $S_{\alpha\beta}(Q)$  of molten NaCl at 875 °C (after Biggin and Enderby [2]).

# **Results and Discussion**

### 1:1 Molten Chlorides

NDIS experiments have been carried out on a number of 1:1 molten metal chlorides to extract the three partial structure factors,  $S_{\alpha\beta}(Q)$  and corresponding PDFs,  $g_{\alpha\beta}(r)$  as described in the previous sections. Table 1 lists their structural properties. The partial structure factors of molten NaCl, which is typical of a molten alkali metal chloride, are shown in Figure 1. As is seen a deep valley in

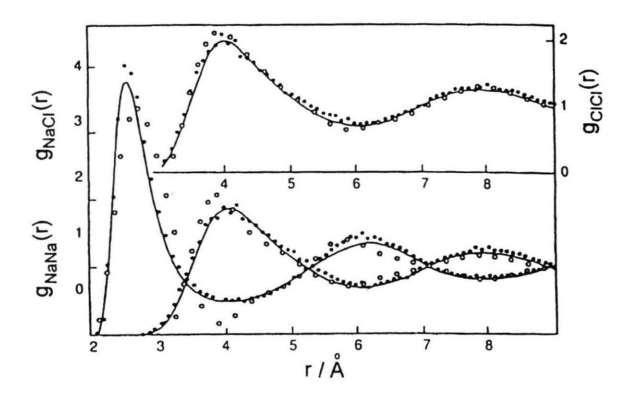


Fig. 2. The pair distribution functions of molten NaCl from neutron diffraction (circles) [2], computer simulation (dots) [32] and liquid-state structural theory (curves [33] (after Ballone et al. [33]).

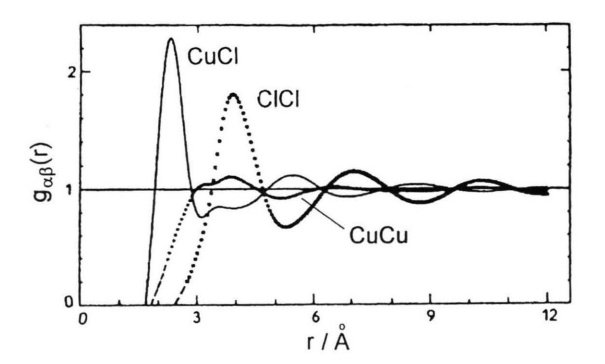


Fig. 3. The pair distribution functions (PDFs) of molten CuCl at 500°C (after Eisenberg et al. [8]).

 $S_{\mathrm{NaCl}}(Q)$  lies in phase with the main peaks in  $S_{\mathrm{NaNa}}(Q)$  and  $S_{\mathrm{ClCl}}(Q)$ , a feature representative of simple Coulombic ordering in 1:1 melts. It needs to be stressed that the pair distribution functions have particular importance since they are accessible to diffraction experiments as well as simulation and theory. Figure 2 compares the cat-

ion-cation, anion-anion and cation-anion PDFs,  $g_{++}(r)$ ,  $g_{--}(r)$  and  $g_{+-}(r)$ , respectively, of molten NaCl determined from NDIS studies [1, 2] with those obtained from MD computer simulations [32] and liquid-state structural theory [33], and the agreement seems to be very good. Figure 2 also shows that  $g_{++}(r)$  and  $g_{--}(r)$  are phased to give complete charge cancellation, a feature characteristic of complete ionisation. Structural properties of molten NaCl, typical of loosely co-ordinated ionic melts, are also representative of other alkali metal chlorides. It is now clear that for such systems theoretical models based on Tosi-Fumi potentials can adequately describe many of the structural features (see e.g., Figure 2).

NDIS work on copper [8, 9] and silver chloride [10] melts indicates that these systems are only weakly ionic with some degree of covalent bonding and a tendency to charge ordering at large distances. These properties tend to favour low co-ordination of first-neighbours. The pair distribution functions of molten CuCl (see Fig. 3) show (i) a featureless cation-cation PDF and corresponding partial structure factor, (ii) a considerable asymmetry between Cu-Cu and Cl-Cl PDFs and, (iii) a deep penetration of Cu<sup>+</sup> ions into the first co-ordination shell of a Cu<sup>+</sup> ion. The gross structural features of these melts can also be reproduced by means of ionic pair potentials, although one notices the need to include polarisation effects.

### 2:1 Molten Chlorides

By adopting the same procedures as for 1:1 chloride melts, NDIS experiments have been performed on a number of 2:1 chloride melts [11–16] such as MgCl<sub>2</sub>, CaCl<sub>2</sub>, SrCl<sub>2</sub>, BaCl<sub>2</sub>, ZnCl<sub>2</sub> and NiCl<sub>2</sub>. Additionally, total ND measurements have been carried out on MnCl<sub>2</sub> [11], and the results show that MgCl<sub>2</sub> and MnCl<sub>2</sub> melts are structurally similar. The structural properties of 2:1 chloride melts are listed in Table 2. Amongst the many important

Table 2. Structural properties of molten 2:1 chloride melts by ND and NDIS techniques.

Salt (Ref.)	T/°C	$r_{c+-}^{a}$	$r_{+-}$	$n_{+-}$	$r_{s+-}^{b}$	$r_{c}^{a}$	r	n	$r_{s}^{b}$	$r_{c++}^{a}$	$r_{++}$	$n_{++}$	$r_{s++}^{b}$	$r_+/{\rm \AA}$	rJr_+_	$r_{\rm p}/{\rm \mathring{A}}^{\rm d}$
ZnCl <sub>2</sub> [15] <sup>c</sup>	327	1.9	2.29	4.3	2.55	3.0	3.71	8.6	3.62	2.8	3.8	4.7	1.48	0.74	1.62	1.03
$ZnCl_2[34]$	330	_	2.29	3.93	2.55	_	3.79	_	3.62	-	_	_	1.48	0.74	1.65	1.005
$ZnCl_2[34]$	600	_	2.31	3.67	2.55	-	3.86	_	3.62	-	-	_	1.48	0.74	1.67	0.944
MgCl <sub>2</sub> [11] <sup>c</sup>	725	_	2.42	4.3	2.47	-	3.56	12	3.62	_	3.81	5	1.32	0.66	1.47	0.93
MnCl <sub>2</sub> [11]	700	_	2.50	4	2.61	-	3.58	8.4	3.62	-	_	_	1.60	0.80	1.43	-
CaCl <sub>2</sub> [12] <sup>c</sup>	820	2.2	2.78	5.4	2.8	2.9	3.73	7.8	3.62	2.7	3.6	4.2	1.98	0.99	1.35	0.95
SrCl <sub>2</sub> [13] <sup>c</sup>	925	2.4	2.9	6.9	2.93	2.4	3.8	9.3	3.62	3.5	4.95	13.6	2.24	1.12	1.35	-
BaCl <sub>2</sub> [14] <sup>c</sup>	1025	1.4	3.1	7.7	3.16	2.5	3.86	7	3.62	3.7	4.9	14	2.70	1.35	1.3	-
NiCl <sub>2</sub> [16] <sup>c</sup>	1022	_	2.36	4.7	2.5	_	3.8	13.8	3.62	_	4.0	6	1.38	0.69	1.61	0.99
NiCl <sub>2</sub> [35]	1050	-	2.28	4.4	2.5	-	3.4	-	3.62	-	-	-	1.38	0.69	1.49	-

<sup>&</sup>lt;sup>a</sup>  $r_c$ =closest distance of approach; <sup>b</sup>  $r_s$ =sum of ionic radii; <sup>c</sup> NDIS technique and all others by ND technique; <sup>d</sup>  $r_p$ =prepeak.

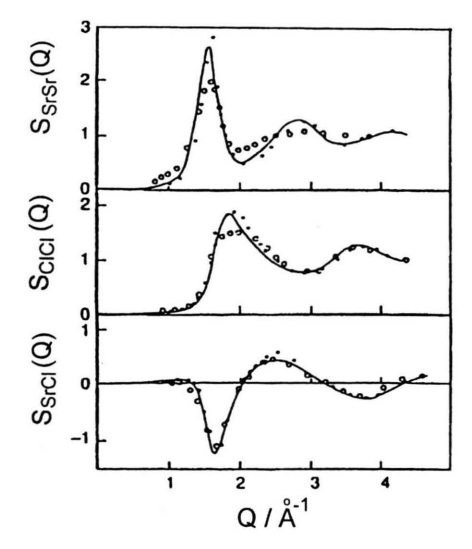


Fig. 4. The partial structure factors of molten  $SrCl_2$  from neutron diffraction (circles) [13], computer simulations (dots) [22] and liquid-state structural theory (curves) [42] (after Pastore et al. [42]).

issues concerning 2:1 chloride melts [11–16, 22, 28, 34-41] are the degree of ionicity and the importance of anionic polarisation in the melt. Figure 4 compares the partial structure factors of molten SrCl<sub>2</sub> determined from NDIS studies [13] with those obtained from computer simulations [22] and liquid-state structural theory [42]. In contrast to the structural features observed in the partial structure factors of molten NaCl (see Fig. 1), the principal peak in  $S_{SrSr}(Q)$  is higher and sharper than that in  $S_{\text{ClCl}}(Q)$  and neither lies in phase with it nor with the valley in  $S_{SrCl}(Q)$ . The main valley in cross-term structure factor,  $S_{SrCl}(Q)$  lies at Q-values intermediate between the positions of principal peaks in like-ion structure factors. Similar behaviour is observed for other alkaline earth metal chlorides such as BaCl<sub>2</sub> [14]. These results suggest that the Coulombic ordering of the two ionic species is to some extent disturbed by the dominant Coulombic repulsions between divalent cations which in this case leads to a cation-cation distance of ~5 Å compared to ~4 Å in molten NaCl. Figure 5 (a) shows the PDFs for molten BaCl<sub>2</sub> and, Fig. 5 (b) compares the PDFs for SrCl<sub>2</sub> obtained from NDIS studies with those obtained from computer simulations [22] and liquid-state structural theory [42]. It can be seen that, although a simple ionic pair-potential (RIM) is still able to explain the broad features of structural ordering in this melt, significant discrepancies at a quantitative level, now appear between the RIM and the NDIS structural data.

The partial structure factors of molten ZnCl<sub>2</sub> are shown in Figure 6. The situation in this melt is quite different from other 2:1 molten salts such as BaCl<sub>2</sub> and SrCl<sub>2</sub>. In contrast to the SrCl<sub>2</sub> case (see Fig. 4), the principal peak in  $S_{CICI}(Q)$  in this case is higher and sharper than that in  $S_{ZnZn}(Q)$ , and the two peaks are now again (as in molten NaCl) in phase with each other and with the valley in the cross-term  $S_{\text{ZnCl}}(Q)$ . However, an additional feature, First Sharp Diffraction Peak, FSDP or a prepeak has now appeared at  $Q \approx 1 \text{ Å}^{-1}$  in all the partial structure factors, more prominently so in the metal-metal term,  $S_{Z_{n}Z_{n}}$ (Q). The appearance of the FSDP has been linked [16, 28, 34, 39, 43, 44] to the existence of Intermediate Range Order (IRO) in the melt. In contrast to the BaCl<sub>2</sub> and SrCl<sub>2</sub> case (see Fig. 5), where penetration effects play a major role in determining both static structure and dynamic behaviour, the PDFs for molten ZnCl<sub>2</sub> also included in Fig. 5 show (i) virtually no penetration of like ions into the first neighbour shells, (ii) that ca. 4 chloride ions surround each zinc ion, (iii) that bond lengths  $r_{\text{Zn-Zn}} = r_{\text{Cl-Cl}}$ and, (iv) no exchange of ions between the 1st shell and the surrounding liquid. The results show the existence of strongly stable local tetrahedral ZnCl<sub>4</sub><sup>2</sup> structural units which form a network via chlorine sharing linkages, thus resulting in a state of pronounced IRO, also indicated by the appearance of the FSDP in the structure factor data. Table 2 and Fig. 5 also reveal an intriguing evolution of short- and intermediate-range order in the structure of 2:1 chloride melts with decreasing cation size.

For example, with decreasing cation size from Ba (1.35 Å), Sr (1.12 Å) and Ca (0.99 Å) to Zn (0.74 Å): (i) the co-ordination number  $n_{+-}$  decreases, respectively, from 7.7, 6.9 and 5.4 to a value of ~4 and, (ii) the first peak in  $g_{++}(r)$  shifts markedly inwards relative to that in  $g_{--}(r)$ . This shift occurs to an extent that in CaCl<sub>2</sub> and ZnCl<sub>2</sub> these peaks are found (see Fig. 5) to coincide, which is contrary to the requirement of maximising the separation of doubly charged cations. Also, the cation-cation partial structure factors show the appearance of the FSDP with decrease of cation size (in Ca, Mg, and Zn), which is regarded as the signature of IRO. Computer simulations based on a simple ionic model (RIM) [45, 46] have failed to reproduce such an evolution of shortand intermediate-range order.

#### 3:1 Molten Chlorides

In comparison to a large number of NDIS investigations on 1:1 and 2:1 halide melts, there is a complete lack of structural data at the PDF level for 3:1 halide

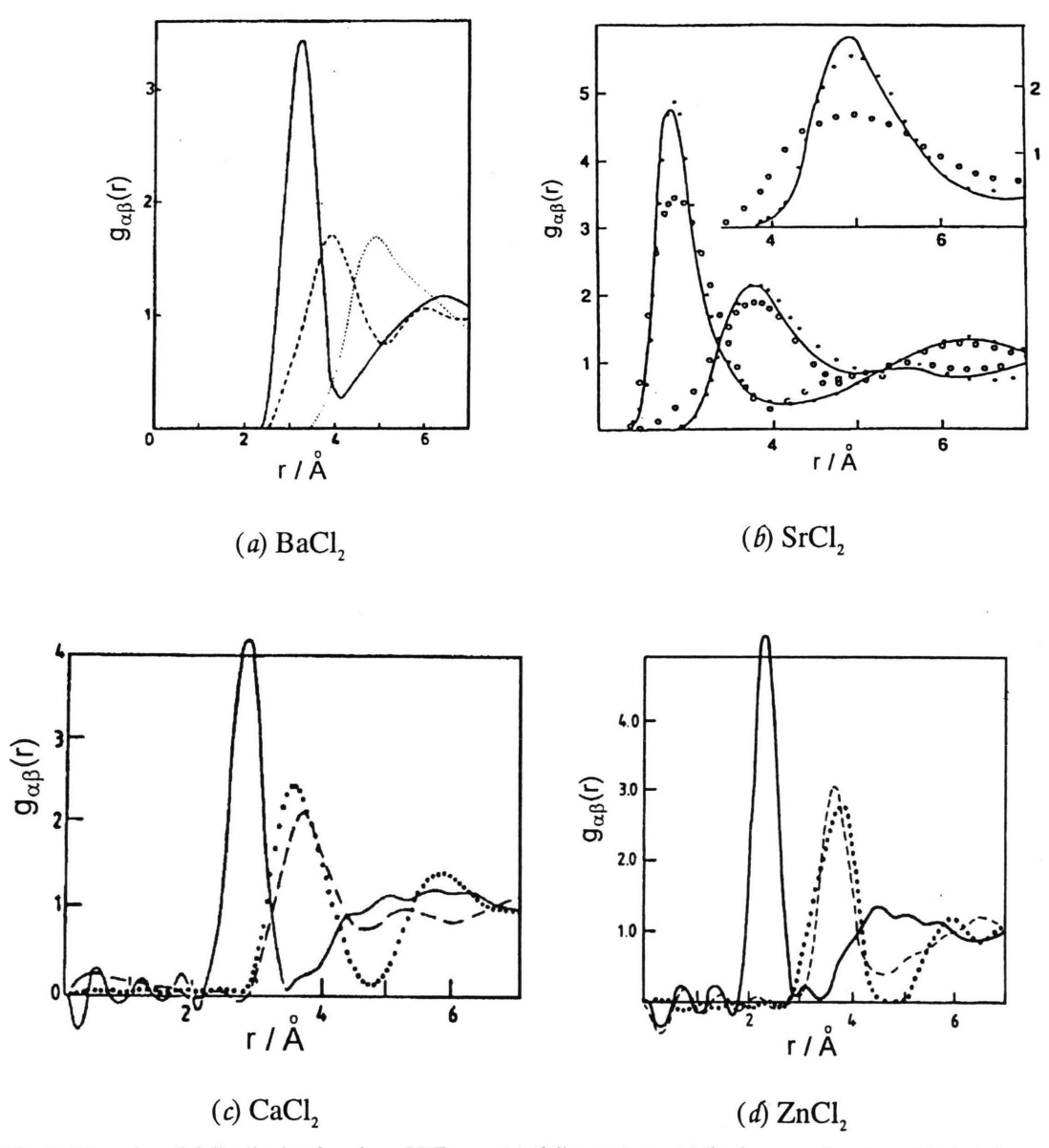


Fig. 5. The pair radial distribution functions, PDFs:  $g_{+-}(r)$  (full curve),  $g_{--}(r)$  (broken curve) and  $g_{++}(r)$  (dotted curve) for molten (a) BaCl<sub>2</sub> [14], (c) CaCl<sub>2</sub> [12] and (d) ZnCl<sub>2</sub> [15]. The RDFs for molten SrCl<sub>2</sub> in (b) from NDIS studies (circles) [13], liquid-state structural theory (curves) [42] and computer simulation (dots) [22]:  $g_{+-}(r)$  (left curves),  $g_{--}(r)$  (right curves) and  $g_{++}(r)$  (inset) (after Pastore et al. [42]).

melts. In fact, whatever structural results have been reported, are at the total structure factor level, and it is true to say that rather little is known as yet about the liquid structure of trivalent metal halides. The trivalent halide salts undergo a variety of structural transitions on melting. Tosi et al. [47–51] have shown in a number of papers that (i) the macroscopic parameters of the melting

transition such as melting temperature,  $T_{\rm m}$ , entropy change,  $\Delta S_{\rm m}$  and fractional volume change  $\Delta V/V_1$ , (ii) the structure of the high-temperature crystal phase before melting and, (iii) the values of transport properties such as ionic conductivity,  $\sigma$  and shear viscosity,  $\eta$  of the melt near freezing are a good indication of structural ordering in molten salts. For clarity of discussion, we first repro-

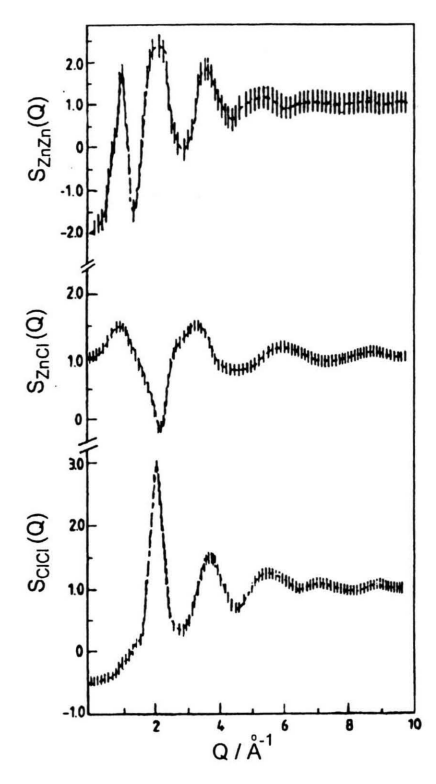


Fig. 6. The partial structure factors,  $S_{\alpha\beta}(Q)$  for molten  $\mathrm{ZnCl}_2$  (after Biggin and Enderby [15]).

Table 3. Physical properties of 3:1 metal chlorides.

Salt	Crystal structure	$T_{\rm m}/(K)$	$\Delta S_{\rm m}/$ (e.u.)	$\Delta V/V_1$	$^{\sigma \prime}_{(\Omega^{-1}cm^{-1})}$	η/ (cp)
SbCl <sub>3</sub>	SbCl <sub>3</sub>	347	8.7	0.17	$2.0 \times 10^{-4}$	_
AlCl <sub>3</sub>	AlCl <sub>3</sub>	466	18.1	0.88	$5.0 \times 10^{-7}$	0.36
FeCl <sub>3</sub>	FeCl <sub>3</sub>	577	17.8	0.39	0.04	-
BiCl <sub>3</sub>	BiCl <sub>3</sub>	507	11.2	0.22	0.38	41.0
InCl <sub>3</sub>	AlCl <sub>3</sub>	859	-	0.61	0.42	-
NdCl <sub>3</sub>	UCl <sub>3</sub>	1032	11.6	0.22	0.60	2.7
YCl <sub>3</sub>	AlCl <sub>3</sub>	994	7.6	0.0045	0.39	_
DyCl <sub>3</sub>	AlCl <sub>3</sub> *	924	6.6	0.0034	0.44	4.2

<sup>\*</sup> High-temperature crystal structure; low-temperature crystal structure is PuBr<sub>3</sub>-type.

duce these properties in Table 3 for all the 3:1 chloride melts investigated so far by the neutron scattering measurements before discussing each one of them.

### SbCl<sub>3</sub>

Triolo and Narten et al. [52, 53] combined neutron and X-ray diffraction data of liquid SbCl<sub>3</sub>, and found that antimony trichloride above its melting temperature is a liquid structured in discrete monomeric molecular units

with an Sb-Cl distance of 2.35 Å. The average arrangement of the discrete units is far from random and, with close intermolecular Sb- -- Cl contacts, results in a very well defined distribution centred around 3.4 Å, a distance much shorter than that expected from van der Waals interactions alone. The results suggest a distorted octahedral arrangement of Cl atoms around each Sb atom in the liguid which has 3 Cl neighbours from other molecules (at 3.4 Å) in addition to the 3 bonded Cl atoms (at 2.35 Å). The structure of the liquid SbCl<sub>3</sub> just above its melting point is described in terms of chains of SbCl<sub>3</sub> molecules stacked in the "umbrella" configurations with the interaction between pairs of molecules within a given chain to be much stronger than the van der Waals forces. However, the interactions between the chains are much weaker.

# AlCl<sub>3</sub>

Badyal et al. [54] performed total ND measurements on molten AlCl<sub>3</sub> and analysed their results by Reverse Monte Carlo (RMC) modelling. The experimental G(r)results show a clear first deep minimum after the well resolved Al-Cl principal peak, thus indicating little movement of anions into and out of the first shell. A co-ordination number  $\bar{n}_{Al}^{Cl} = 4$  along with a value of  $r_{-}/r_{+} = 1.66$ establishes a regular four-fold coordinated tetrahedral geometry in molten AlCl<sub>3</sub>. Harris et al. [55] from their X-ray diffraction measurements suggest a structural model for molten AlCl<sub>3</sub> as consisting of discrete Al<sub>2</sub>Cl<sub>6</sub> dimers, each formed by edge sharing of two distorted AlCl<sub>4</sub> tetrahedra. However, in contradiction to this model, Badyal et al. [54] observe predominantly chains of mainly corner-linked tetrahedral units with only partial dimerisation, and propose a "sparse network liquid" model for molten AlCl<sub>3</sub>. Since ZnCl<sub>2</sub> and AlCl<sub>3</sub> have some intriguing similarities in their physical properties such as a low melting point and very low conductivity in the melt, they suggest that the structure of molten AlCl<sub>3</sub> is similar to that of the network ZnCl2 melt with the difference that in AlCl<sub>3</sub> there is much less connectivity. This seems plausible since a 3:1 salt should require less anion sharing than a 2:1 salt for achieving four-fold co-ordination. The melting of AlCl<sub>3</sub> from an ionic layer structure into a molecular liquid of Al<sub>2</sub>Cl<sub>6</sub> units is accompanied (see Table 3) by low  $T_{\rm m}$ , very large values of  $\Delta S_{\rm m}$ and  $\Delta V/V_1$ , a very low value of  $\sigma$  in the melt and a rather low value of  $\eta$ . The large increase (~88%) in fractional volume on melting is explained in terms of the dramatic change in the co-ordination of Al3+ ion from octahedral in the crystal [56] to tetrahedral [54, 55] in the melt.

### FeCl<sub>3</sub>

FeCl<sub>3</sub> shows an anomalously high increase of entropy and volume change on melting similar to that in AlCl<sub>3</sub>, and this behaviour contrasts dramatically with YCl<sub>3</sub> (see Table 3). The total ND measurements on molten FeCl<sub>3</sub> [57, 58] combined with model calculations and computer simulations indicate that melting in this case is accompanied by a change in the local structure from the octahedral environment of the Fe<sup>3+</sup> ions in the crystal to a tetrahedral environment where Fe<sub>2</sub>Cl<sub>6</sub> molecular units exhibit substantial intermolecular correlations. This behaviour is similar to that observed in AlCl<sub>3</sub> but in contrast to that of YCl<sub>3</sub> (see later) where octahedral co-ordination of Y is preserved on melting.

### BiCl<sub>3</sub>

Fukushima et al. [59] performed time-of-flight ND measurements on bismuth trihalides,  $BiX_3$  (X=Cl, Br, I) at a number of temperatures and concluded that the pure molten  $BiX_3$  system behaves like a molecular liquid similar to  $PX_3$ . The results of total ND measurements performed on molten  $BiCl_3$  at 300 °C by Price et al. [49] indicate a metal ion co-ordination of ~3, thus suggesting a molecular configuration in the melt. If monomers are the basic constituents in this liquid, they should be strongly interacting to allow relatively fast exchange of the halogen ions, in accord with the observed ionic conductivity (see Table 3) of the melt which is appreciable.

## InCl<sub>3</sub>

InCl<sub>3</sub> has the AlCl<sub>3</sub> structure in the crystal and its volume change on melting is large. However, both its melting temperature and ionic conductivity are similar to YCl<sub>3</sub> rather than AlCl<sub>3</sub>. From the total ND measurements on molten InCl<sub>3</sub> which yielded a metal-chlorine co-ordination between 5 and 6, Price et al. [49] suggested (i) a partial survival of the network structure in the melt which is in contrast to the low metal-ion coordination in BiCl<sub>3</sub> indicative of formation of BiCl<sub>3</sub> or Bi<sub>2</sub>Cl<sub>6</sub> molecular units and, (ii) that the nature of the structure and bonding of InCl<sub>3</sub> and BiCl<sub>3</sub> is intermediate between the well defined molecular configurations of AlCl<sub>3</sub> and FeCl<sub>3</sub> on one hand and the network structure of YCl<sub>3</sub> (see later) on the other.

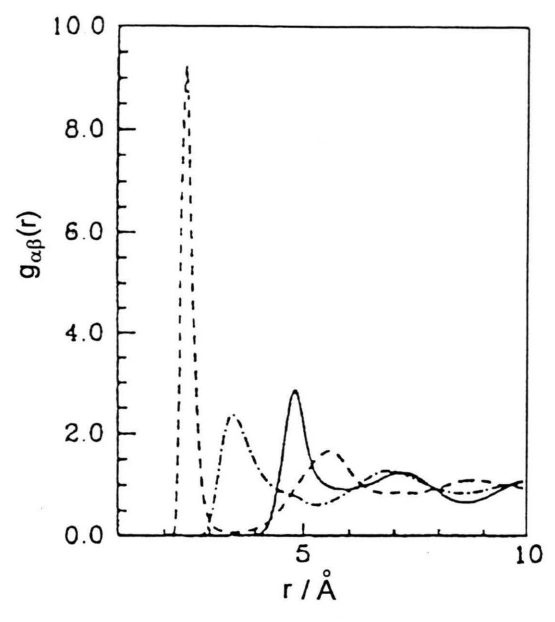
### NdCl<sub>3</sub>

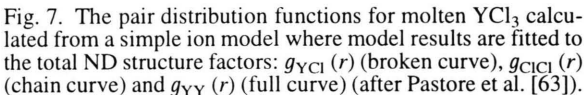
In the solid state, NdCl<sub>3</sub> crystallises in the UCl<sub>3</sub>-type structure (also known as Y (OH)<sub>3</sub>-type structure) which may be described as hexagonal with each U surrounded by six Cl on the corners of a trigonal prism and further co-ordinated by three coplanar Cl at somewhat larger distance. Saboungi et al. [60] used X-ray data of Mochinaga et al. [25, 26] in conjunction with their total ND results to obtain a model structure using the RMC modelling. The results did not provide structural details of much significance. However, from the similarity of the RMC generated triplet correlation functions for the liquid with those in the crystalline state, the authors suggested that the local structure in the melt, although considerably more disordered than in the solid, still remains some characteristics of the solid phase. Also, the presence of a FSDP in the total structure factor at  $\sim 1 \text{ Å}^{-1}$  indicates the existence of IRO in this melt.

# YC13

YCl<sub>3</sub> is structurally isomorphous to AlCl<sub>3</sub> in the crystalline state but the two compounds show entirely different melting mechanisms, with very different values for their melting and transport properties. YCl3 crystal melts with a relatively moderate entropy change and an essentially negligible volume change. ND results for molten YCl<sub>3</sub> [50, 61] show (i) the existence of a FSDP (at  $Q \approx 0.95 \text{ Å}^{-1}$ ) associated with IRO in the melt and, (ii) a co-ordination number for Cl about Y of 5.9, thus confirming an octahedral co-ordination for Y which agrees with the Raman scattering findings [62] of rather longlived octahedral structural units. Tosi et al. [63] performed liquid structure calculations for an ionic model of molten YCl<sub>3</sub>. After obtaining a reasonable agreement between their calculated and experimental total ND functions, they reported the calculated partial structure factors and pair distribution functions shown in Figure 7. The results indicate melting of YCl<sub>3</sub> into a loose ionic network structure formed by edge-sharing octahedra with the presence of an IRO while in molten AlCl<sub>3</sub>, as we have already seen, molecular dimers composed of edge-sharing [55] or corner-linked [54] tetrahedral units are formed. The difference in the melting behaviour of AlCl<sub>3</sub> and YCl3 is thus related to the relative stability of tetrahedral and octahedral co-ordinations and, reflects subtle difference in the balance between ionic and covalent components of bonding.

Tosi et al. [48, 51] classified the melting mechanism of trichlorides as being of three main types: molecular-





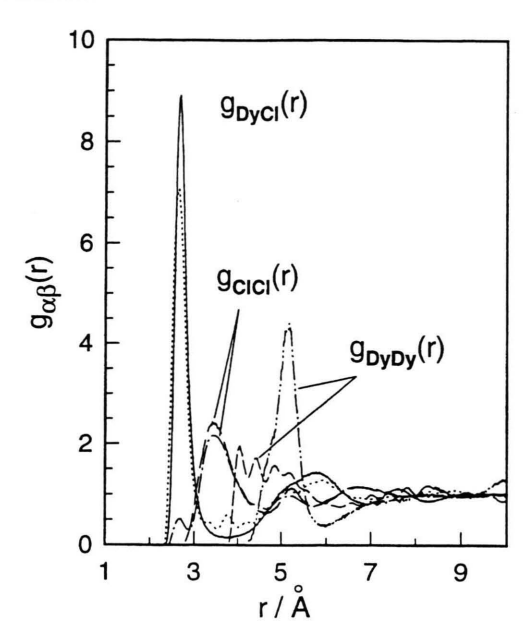


Fig. 8. Comparison of the three PDFs for molten DyCl<sub>3</sub> obtained experimentally using the NDIS technique (lower curves) with those simulated (higher curves) using the Rigid Ion Model (RIM) potentials.

to-molecular, ionic-to-molecular and ionic-to-ionic exemplified, respectively by SbCl<sub>3</sub>, AlCl<sub>3</sub> and YCl<sub>3</sub>, which are some of the trichlorides investigated by ND studies.

# DyCl<sub>3</sub>

DyCl<sub>3</sub> transforms into AlCl<sub>3</sub> structure before melting where it is structurally isomorphous to YCl<sub>3</sub> and melts with similarly low values of  $\Delta S_{\rm m}$  and  $\Delta V/V_{\rm l}$ . From the proximity of Dy to Y in Pettifor's chemical scale, Tosi et al. [50] suggested that DyCl<sub>3</sub> should show similar melting mechanism and liquid structure as YCl<sub>3</sub>.

Molten DyCl<sub>3</sub> is the first and only trivalent halide system in which isotopic substitution technique of neutron diffraction (NDIS) has been used [27] to extract the three partial pair distribution functions, PDFs. Figure 8 compares the three PDFs determined experimentally with those simulated using a rigid ion model. The simulated results are broadly in agreement with the NDIS results suggesting a six-fold co-ordination of Cl around Dy and a stable geometry for DyCl<sub>6</sub><sup>3</sup> octahedra existing on a short-range in the melt. A detailed comparison at the PDF level (Fig. 8) reveals that although  $g_{\text{Dy-Cl}}(r)$  and  $g_{\text{Cl-Cl}}(r)$  are well represented by MD simulations with a RIM, certain discrepancies in the  $g_{\text{Dy-Dy}}(r)$  are still

present. The NDIS experimental results show that the 1st peak in  $g_{Dy-Dy}(r)$  is split into component distances corresponding to face-, edge- and apex-sharing octahedral configurations. MD simulations based on RIM seem to reproduce the edge- and apex-sharing configurations but not the face-sharing ones. Recently, Wilson and Madden [28] proposed a polarisable ion model (PIM) to explain the intriguing structural evolution in 2:1 halide melts with decreasing cation size. According to this model, ions are not simply charged hard spheres; their properties change profoundly with their environment and, they may undergo polarisation and dispersion interactions. The situation for octahedral co-ordination of metal ions is illustrated in Fig. 9 where the dipole induced by the cations on the anion effectively interposes a negative charge along the line of centres between the two cations. The cation-cation repulsive Coulomb interactions get screened by the polarisable ions thus accounting for short cationcation separations as observed in  $g_{Dy-Dy}(r)$ . Figure 9 illustrates that polarisability, especially for small and highly charged cations such as Dy<sup>3+</sup>, could favour the formation of rings of intermediate size which could be associated with the prepeak (FSDP) observed in the structure factor data. The total structure factors for the three isotopic samples of DyCl<sub>3</sub> show [27] that the main or pre-

Fig. 9. An illustration of polarisable ion model (PIM) for octahedral co-ordination of metal ions,  $Dy^{3+}$  (small circles) with  $Cl^-$  (large circles). The dipole induced by the cation on the anion effectively interposes a negative charge along the line of centers between two cations and, Dy-Cl-Dy bond bending leads to corner-sharing (I), edge-sharing (II) and face-sharing (III) octahedra

dominant contribution to the FSDP at  $Q \approx 1 \text{ Å}^{-1}$  is the metal-metal term, and these Dy-Dy correlations exist on the scale of IRO through chlorine sharing linkages. While the RIM and PIM simulated PDFs,  $g_{\text{Dy-Cl}}(r)$  and  $g_{\text{Cl-Cl}}(r)$  reproduce [29] equally well the experimental PDFs and have similar shapes from the two models, the results for Dy-Dy partial PDF obtained from the two models (see Fig. 10) are quite different. There is excellent agreement of experimental  $g_{\text{Dy-Dy}}(r)$  with the PIM result and, these results highlight the importance of including polarisation effects in the model potential used for simulations. The

above results show that (i) the distribution of anions is hardly affected by the polarisation effects and, (ii) although repulsion between triply charged Dy<sup>3+</sup> ions should maximise the separation between the cations, this effect is offset by the polarisation of anions by highly charged cations, thus leading to shortened cation-cation distances due to Dy-Cl-Dy "bond bending", as illustrated in Figure 9. The results also show that molten DyCl<sub>3</sub> has a network structure with corner-, edge- and face-sharing octahedral units, although the face-sharing units are present in only a very small fraction.

DyCl<sub>3</sub> and YCl<sub>3</sub> are predicted [50] to be isomorphous in their liquid state. However, a comparison (see Figs. 7 and 8) of the PDFs obtained from a simple ion model (RIM) of molten YCl<sub>3</sub>, where model results [63] are fitted to the total ND results [50, 61], with those for molten DyCl<sub>3</sub> obtained by fitting RIM results [29-31] to the three partials obtained by NDIS technique [27], clearly shows that the two results are different. In this respect it is worth mentioning that, when we used the potential parameters for DyCl<sub>3</sub> after obtaining a satisfactory agreement between the simulated and experimental total structure functions, the predicted mixing enthalpies for the binary melts, x DyCl<sub>3</sub>+(1-x) NaCl were found [64] to be an order of magnitude different from those determined experimentally by calorimetric methods. However, with the revised potential parameters for DyCl<sub>3</sub>, which were readjusted [29-31] to obtain satisfactory agreement between the three simulated and experimental partial structure factors in pure molten DyCl<sub>3</sub>, the experimental mixing enthalpies for the binary melts are reasonably repro-

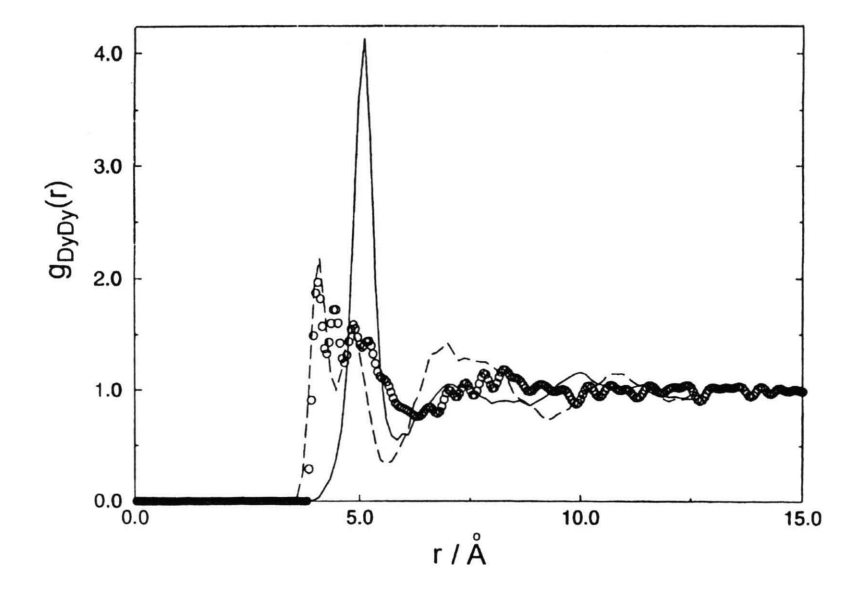


Fig. 10. Comparison of the pair radial distribution function,  $g_{\rm Dy-Dy}(r)$  in molten DyCl<sub>3</sub> calculated by using PIM and RIM potentials along with the one obtained from experimental NDIS studies: solid line (RIM result), dashed line (PIM result) and open circles (experimental data).

duced even with the RIM, without invoking polarisation effects.

#### **Conclusions**

The above discussion shows that the total ND measurements for 3:1 halide melts do not provide structural details of much significance. If comparison between simulations and diffraction experiments are to be made, this should be done, wherever possible, at the pair distribution function (PDF) level. The techniques of neutron diffraction isotopic substitution (NDIS) in conjunction with computer simulations and liquid-state structural theory will continue to play a significant role in deepening our understanding of molten salts and their binary mixtures. However, due to certain limitations in the use of NDIS techniques such as prohibitive costs, high absorption cross-sections, large neutron resonances and small contrast variations of certain isotopes, greater use will be made in the next decade of combining neutrons and Xray data. With the development of new powerful X-ray sources such as ESRF at Grenoble, Photon factory at Argonne, this is already beginning to happen.

Molten DyCl<sub>3</sub> is the first 3:1 halide melt in which PDFs have been obtained experimentally by the isotopic substitution technique of neutron diffraction (NDIS). A comparison between polarisable ion model (PIM) and rigid ion model (RIM) simulated results for this system highlights the importance of including polarisation effects into the model potentials. Molten DyCl<sub>3</sub> is found to have a network structure with corner-, edge- and facesharing octahedral DyCl<sub>6</sub><sup>3</sup> units, although the face-sharing units are present in only a very small fraction.

### Acknowledgements

We thank our many colleagues and collaborators to whose work we have referred in the preceeding pages. We are particularly grateful to Professor John Enderby for his enthusiastic support and critical comments on many of the neutron results. We acknowledge our coworkers and collaborators, in particular Drs. A. C. Barnes (University of Bristol), H. Fischer (ILL, France), Prof. P. A. Madden, and Mr. F. Hutchinson (University of Oxford), Prof. Y. Sato (Tohoku University, Japan), Mr. M. Sakurai (TIT, Japan), Dr. O. N. Kalugin, Mr. L. Bianchi, and Mr. M. Shcherbakov (University of Abertay Dundee) for their help and, for access to unpublished or aboutto-be published results. AKA wishes to acknowledge the hospitality extended to him by the IUSTI, Marseilles (France) during the summer of 1998 when this work was written up. Finally we thank the Engineering and Physical Sciences Research Council, EPSRC (UK), Monbusho and Tokyo Electric Company, Japan for their continued support of our research programme.

- [1] F. G. Edwards, J. E. Enderby, R. A. Howe, and D. I. Page, J. Phys. C: Solid State Phys. 8, 3483 (1975).
- [2] S. Biggin and J. E. Enderby, J. Phys. C: Solid State Phys. **15,** L305 (1982).
- [3] R. L. McGreevy and M. A. Howe, J. Phys.: Condens. Matter 1, 9957 (1989).
- [4] M. A. Howe and R. L. McGreevy, Phil. Mag. B 58, 485 (1988).
- [5] J. Y. Derrien and J. Dupuy, J. Phys., Paris **36**, 191 (1975).
- [6] E. W. J. Mitchell, P. F. J. Poncet, and R. J. Stewart, Phil. Mag. B 34, 721 (1976).
- [7] J. Locke, S. Messoloras, R. J. Stewart, R. L. McGreevy, and E. W. J. Mitchell, Phil. Mag. B 51, 301 (1985).
- [8] S. Eisenberg, J.-F. Jal, J. Dupuy, P. Chieux, and W. Knoll, Phil. Mag. A 46, 195 (1982).
- [9] D. I. Page and K. Mika, J. Phys. C4, 3034 (1971).
- [10] J. Y. Derrien and J. Dupuy, Phys. Chem. Liq. 5, 71 (1976).
- [11] S. Biggin, M. Gay, and J. E. Enderby, J. Phys. C: Solid State Phys. 17, 977 (1984). [12] S. Biggin and J. E. Enderby, J. Phys. C: Solid State Phys.
- **14,** 3577 (1981).
- [13] R. L. McGreevy and E. W. J. Mitchell, J. Phys. C 15, 5537
- [14] F. G. Edwards, R. A. Howe, J. E. Enderby, and D. I. Page, J. Phys. C: Solid State Phys. 11, 1053 (1978).
- [15] S. Biggin and J. E. Enderby, J. Phys. C: Solid State Phys. **14,** 3129 (1981).

- [16] R. J. Newport, R. A. Howe, and N. D. Wood, J. Phys. C: Solid State Phys. 18, 5249 (1985).
- [17] L. Koester, K. Knopf, and K. Waschkowski, Z. Phys. A 282, 371 (1977).
- [18] L. V. Woodcock and K. Singer, Trans. Faraday Soc. 67, 12 (1971).
- [19] M. Dixon and M. J. L. Sangster, J. Phys. C 8, L 8 (1975);
- 9, L 5 (1976); 9, 909 (1976).
- [20] M. Dixon and M. J. Gillan, Phil. Mag. B 43, 1099 (1981).
- [21] M. J. L. Sangster and M. Dixon, Adv. Phys. 25, 247 (1976).
- [22] S. de Leeuw, Molec. Phys. **36**, 103 and 765 (1978)
- [23] A. Baranyai, I. Ruff, and R. L. McGreevy, J. Phys. C: Solid State Phys. 19, 453 (1986).
- [24] J. Mochinaga, Y. Miyagi, K. Igarashi, K. Fukushima, and Y. Iwadate, J. Chem. Soc. Japan, 5, 459 (1993).
- [25] J. Mochinaga, Y. Iwadate, and K. Fukushima, "Molten Salt Chem. Tech.", Materials Science Forum, ed. M. Chemla, D. Devilliers, Trans. Tech. Pub. Ltd., Zürich 73–75, 147 (1991).
- [26] H. Ohno, K. Igarashi, N. Umesaki, and K. Furukawa, "Xray Diffraction Analysis of Ionic Liquids", Molten Salt Forum, Trans Tech. Pub. Ltd., Zürich, 3, 1 (1994).
- [27] A. K. Adya, R. Takagi, Y. Sato, M. Gaune-Escard, A. C. Barnes, and H. Fischer, J. Chem. Phys., to be submit-
- [28] M. Wilson and P. A. Madden, J. Phys.: Condens. Matter **5,** 6833 (1993); **6,** 159 (1994).

- [29] R. Takagi, F. Hutchinson, P. A. Madden, A. K. Adya, and M. Gaune-Escard, J. Phys.: Condens. Matter, 11, 645 (1999).
- [30] M. Sakurai, R. Takagi, A. K. Adya, and M. Gaune-Escard, Z. Naturforsch. 53a, 655 (1998).
- [31] A. K. Adya, R. Takagi, M. Sakurai, and M. Gaune-Escard, Proc. 11th Int. Symp. Molten Salts, ed. P. C. Trulove, H. De Long, and S. Deki, Electrochem. Soc. Inc., Pennington 98 (1998) in press.
- [32] J. W. Lewis, K. Singer, and L. V. Woodcock, J. Chem. Soc. Faraday Trans. 271, 41 (1975).
- [33] P. Ballone, G. Pastore, and M. P. Tosi, J. Chem. Phys. 81, 3174 (1984).
- [34] D. A. Allen, R. A. Howe, N. D. Wood, and W. S. Howells, J. Chem. Phys. 94, 5071 (1991).
- [35] Y. S. Badyal and Ř. A. Howe, J. Phys.: Condens. Matter **5**, 7189 (1993).
- [36] S. E. Day and R. L. McGreevy, Phys. Chem. Liq. 15, 129 (1985).
- [37] M. C. Fairbanks, M. A. Howe, and R. L. McGreevy, Phys. Chem. Liq. 18, 179 (1988).
- [38] R. L. McGreevy, Solid State Phys. 40, 247 (1987).
- [39] N. D. Wood and R. A. Howe, J. Phys. C: Solid State Phys. **21**, 3177 (1988).
- [40] N. D. Wood, R. A. Howe, R. J. Newport, and J. Faber Jr., J. Phys. C: Solid State Phys. 21, 669 (1988).
- [41] R. L. McGreevy and L. Pusztai, Proc. Roy. Soc. London A **430**, 241 (1990).
- [42] G. Pastore, P. Ballone, and M. P. Tosi, J. Phys. C: Solid State Phys. 19, 487 (1986).
- [43] P. S. Salmon, Proc. Roy. Soc. London A 437, 591 (1992).
- [44] P. S. Salmon, Proc. Roy. Soc. London A 445, 351 (1994).
- [45] L. V. Woodcock, C. A. Angell, and P. Cheeseman, J. Chem. Phys. 65, 1565 (1976).
- [46] P. J. Gardner and D. M. Heyes, Physica B 113, 227 (1985).
- [47] M. P. Tosi, J. Phys.: Condens. Matter 6, A13 (1994).

- [48] M. P. Tosi, Z. Phys. Chem. 184, 121 (1994).
- [49] D. L. Price, M. L. Saboungi, W. S. Howells, and M. P. Tosi, Proc. Int. Symp. Molten Salts, ed. M. L. Saboungi and H. Kojima, Electrochem. Soc. Inc., Pennington 93-9, 1 (1993).
- [50] M. P. Tosi, G. Pastore, M. L. Saboungi, and D. L. Price, Physica Scripta T39, 367 (1991).
- [51] M. P. Tosi, D. L. Price, and M. L. Saboungi, Ann. Rev. Phys. Chem. 44, 173 (1993).
- [52] R. Triolo and A. H. Narten, J. Chem. Phys. 69, 3159 (1978).
- [53] E. Johnson, A. H. Narten, W. E. Thiessen, and R. Triolo, Farad. Discuss. Chem. Soc. 66, 287 (1978).
- [54] Y. S. Badyal, D. A. Allen, and R. A. Howe, J. Phys.: Condens. Matter 6, 10193 (1994).
- [55] R. L. Harris, R. E. Wood, and H. L. Ritter, J. Amer. Chem. Soc. 73, 3151 (1951).
- [56] K. N. Semenenko and T. N. Naamova, Russ. J. Inorg. Chem. 9, 718 (1964).
- [57] D. L. Price, M. L. Saboungi, S. Hashimoto, and S. C. Moss, Proc. 8th Int. Symp. Molten Salts, ed. R. J. Gale, G. Blomgren and H. Kojima, Electrochem. Soc. Inc., Pennington 92-16, 14 (1992).
- [58] D. L. Price, M. L. Saboungi, Y. S. Badyal, J. Wang, S. C. Moss, and R. L. Leheny, Phys. Rev. B 57, 10496 (1998).
- [59] Y. Fukushima, M. Misawa, and K. Suzuki, Res. Rep. Lab. Nucl. Sci. (Tohoku University) 8, 113 (1975).
- [60] M. L. Saboungi, M. A. Howe, and D. L. Price, Proc. 7th Int. Symp. Molten Salts, ed. C. L. Hussey, S. N. Flengas, J. S. Wilkes, and Y. Ito, Electrochem. Soc. Inc., Pennington 90-17, 8 (1990).
- [61] M. L. Saboungi, D. L. Price, C. Scamehorn, and M. P. Tosi, Europhys. Lett., 15, 283 (1991).
- [62] G. N. Papatheodorou, J. Chem. Phys. 66, 2893 (1977).
- [63] G. Pastore, Z. Akdeniz, and M. P. Tosi, J. Phys.: Condens. Matter 3, 8297 (1991).
- [64] R. Takagi, L. Rycerz, and M. Gaune-Escard, Denki Kagaku 62, 1994 (1994).